Fourier-space generation of abruptly autofocusing beams and optical bottle beams

Ioannis Chremmos,[1,*] Peng Zhang,[2,3] Jai Prakash,[2] Nikolaos K. Efremidis,[1] Demetrios N. Christodoulides,[4] and Zhigang Chen[2]

[1]*Department of Applied Mathematics, University of Crete, Heraklion 71409, Crete, Greece*

[2]*Department of Physics and Astronomy, San Francisco State University, San Francisco, California 94132, USA*

[3]*NSF Nanoscale Science and Engineering Center, University of California, Berkeley, California 94720, USA*

[4]*CREOL/College of Optics, University of Central Florida, Orlando, Florida 32816, USA*

**Corresponding author: jochremm@central.ntua.gr*

Received July 19, 2011; accepted August 15, 2011;
posted August 24, 2011 (Doc. ID 151378); published September 14, 2011

We demonstrate analytically and experimentally that a circular abruptly autofocusing (AAF) Airy beam can be generated by Fourier-transforming an appropriately apodized Bessel beam whose radial oscillations are chirped by a cubic phase term. Depending on the relation between the chirp rate and the focal distance of the Fourier-transforming lens, it is possible to generate AAF beams with one or two foci, the latter case leading to the formation of an elegant paraboloid optical bottle. © 2011 Optical Society of America

OCIS codes: 050.1940, 260.2030, 350.5500.

Abruptly autofocusing (AAF) beams constitute a newly introduced species of $(2+1)$D light waves that are able to focus their power right before a target is reached [1]. Circular Airy beams (CAB), i.e. circularly symmetric beams with Airy radial profile, were the first AAF beams to be proposed. Because of the inward, diffraction-resisting radial acceleration of the Airy wave function, the beam's intensity rings contract towards the axis with minimum shape distortion, hence keeping the maximum intensity constant along the entire path between source and focus. The main (inner) intensity ring writes a paraboloid caustic surface of revolution in space that collapses on-axis at a point of maximum amplitude gradient, right before the intended focus [2]. As was first predicted theoretically [1] and subsequently observed experimentally [3,4], these properties allow AAF beams to achieve power delivery within smaller focal volumes and at longer focal distances, as compared to classic Gaussian beams of comparable initial width. For these reasons, AAF waves are envisaged to find major applications in laser medicine and other linear or nonlinear optical settings.

An optical beam can be generated either directly in the real space or indirectly in the Fourier-space. In the latter case, the Fourier-transform (FT) of the beam is generated first and then Fourier-transformed back into the real space by a lens. This technique has been especially successful for 1D and 2D finite-energy Airy beams, whose FT is known analytically [5]. Unfortunately, so far no analytical expression has been found for the FT of a CAB and hence its generation relies on the numerically computed FT.

In this Letter, a highly accurate closed-form expression is reported for the FT of a CAB. Through asymptotic analysis, we show that the FT behaves like a J_0 Bessel function that oscillates with a quadratic chirp rate due to an additional cubic phase term. The FT amplitude is apodized by the product of a Gaussian function with another function that scales quadratically. The derived FT can be used to define beams that evolve into AAF beams with desired characteristics after being Fourier-transformed by a thin lens. We show that, depending on the relation between the chirp rate and the lens' focal distance, an AAF beam can have one or two foci. In the second case, the two foci are symmetric with respect to the lens' focal plane, thus creating an elegant optical bottle with paraboloid multilayer boundaries and two closed ends. Experimentally, we successfully demonstrate such an optical bottle using a CAB. Our finding also explains the morphing of AAF beams to expanding Bessel-like beams in the Fraunhofer region [6,7]. Moreover, knowledge of the FT provides control over the transition from CABs into Bessel-like beams or optical bottle beams, that can be very useful in particle guiding and trapping applications [7–9].

To begin, consider the input amplitude of a CAB

$$u(r) = Ai(r_0 - r)\exp[a(r_0 - r)], \tag{1}$$

where r is the scaled polar distance, $r_0 + 1$ is approximately the radius of the main ring and a is the apodization rate. The (2D) FT of this circularly symmetric wavefront is expressed as a Hankel-transform integral

$$U(k) = \int_0^\infty u(x)J_0(kx)x\mathrm{d}x. \tag{2}$$

The key assumption to our derivation is that, if r_0 is sufficiently large, this integral can be extended to $-\infty$ without affecting the result, because of the strongly decaying Airy function. Alternatively, using the slightly modified initial condition $u(r) - u(-r)$, the above integral goes from $-\infty$ to ∞. By introducing the function $g(x) = (r_0 - x)Ai(x)\exp(ax)$, Eq. (2) becomes a convolution integral, which by the convolution theorem, becomes

$$U(k) = \frac{1}{2\pi}\int_{-\infty}^{\infty} G(\omega)W(\omega, k)e^{i\omega r_0}\mathrm{d}\omega, \tag{3}$$

where G and W are, respectively, the 1D FTs of functions $g(x)$ and $J_0(kx)$, which are known in closed form:

 © 2011 Optical Society of America

$$G(\omega) = [r_0 + (\omega + ia)^2]\exp[i(\omega + ia)^3/3],$$
$$W(\omega) = \begin{cases} 2(k^2 - \omega^2)^{-1/2}, & |\omega| < k \\ 0, & |\omega| > k \end{cases}. \quad (4)$$

Note that, to derive $G(\omega)$ we have used the FT of the finite-power 1D Airy beam [5]. Since $W(\omega)$ vanishes for $|\omega| > k$, the integral of Eq. (3) is essentially carried out over the finite interval $(-k, k)$. Changing the integration variable by $\omega = k\cos\varphi$we obtain

$$U(k) = \int_0^{\pi} F(\varphi)e^{iQ(\varphi)}\mathrm{d}\varphi, \quad (5)$$

where

$$\pi F(\varphi) = [r_0 + (k\cos\varphi + ia)^2]\exp(a^3/3 - ak^2\cos^2\varphi),$$
$$Q(\varphi) = (k^3/3)\cos^3\varphi + k(r_0 - a^2)\cos\varphi. \quad (6)$$

Equation (5) is very convenient because the integrand oscillates rapidly with increasing k, suggesting a stationary-phase approach with k being the large parameter required. There are two stationary points, namely $\varphi = 0, \pi$, whose total contribution is

$$U^{SP}(k) = \sqrt{\frac{2\pi}{-Q''(0)}}\mathrm{Re}[F(0)\exp(iQ(0) - i\pi/4)], \quad (7)$$

where $Q''(0) = -k^3 - k(r_0 - a^2)$. A comparison of Eq. (7) with the result obtained by numerically integrating Eq. (2) reveals its high accuracy even for $k < 1$. In fact, the only shortcoming of Eq. (7) seems to be its divergent $k^{-1/2}$ behavior as $k \to 0$. The correct limit for $k \to 0$ is obtained from Eq. (2), using the integral representation of Bessel function and equals $(r_0 - a^2)J_0[(r_0 - a^2)k]$ or $\approx r_0 J_0(kr_0)$, since the apodization rate is normally small (order of 0.1). Now, in order to combine the two obtained asymptotic expressions into a uniform one, we define the function

$$V(k) = (r_0 + k^2)e^{-ak^2}\sqrt{\frac{kr_0 + k^3/3}{kr_0 + k^3}}J_0(kr_0 + k^3/3), \quad (8)$$

which is easily shown to behave correctly in both limits. Indeed, for $k \to 0$, $V(k) \to r_0 J_0(kr_0)$, while, for large k, it agrees with Eq. (7), taking into account the asymptotic expression $J_0(x) \approx \sqrt{2/\pi x}\cos(x - \pi/4)$, and assuming a small a so that $\mathrm{Im}\{F(0)\}$ can be ignored. Moreover, it turns out that the accuracy of Eq. (8) is surprisingly high throughout the spectrum, as deduced by comparing it to the numerically computed FT from Eq. (2). An example is shown in Fig. 1(a) for a typical CAB.

Equation (8) is a central result to this Letter, being the first closed-form approximation reported for the FT of a CAB. The FT behaves proportionally to a J_0 Bessel function whose phase is enhanced by a cubic term, i.e. it oscillates with a quadratic chirp rate. The FT amplitude is modulated by a function that scales quadratically and apodized by a Gaussian function that decays faster with increasing decay rate a. There is an additional

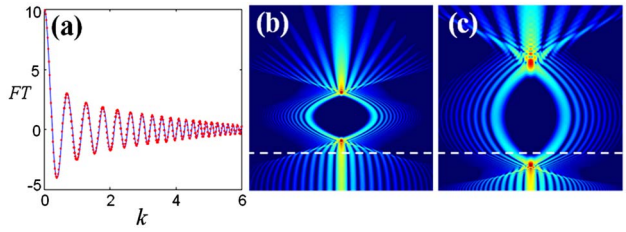

Fig. 1. (Color online) (a) FT of a CAB with $r_0 = 10, a = 0.05$, as given by Eq. (2) (blue line) and by Eq. (8) (red dots). (b),(c) Full-wave simulation of CABs generated by Fourier–transforming chirped Bessel beams. The dashed lines indicate the lens with $f = 10$. $c = 10$ in (b) and $C = 6$ in (c), while $a = 0.05$.

square-root factor that varies monotonically from 1 to $3^{-1/2}$. For an ideal infinite-power CAB ($a = 0$), the FT envelope diverges at infinity as $k^{1/2}$.

The morphing of AAF beams into Bessel-like beams in the far-field is now fully understood: For beams propagating according to the scaled paraxial equation $2u_z = i\nabla_t^2 u$, the wave amplitude in the Fraunhofer region is $u(r, z) = \exp(ir^2/2z)U(r/z)/iz$, where U is the FT of $u(r, 0)$. After Eq. (8), the far-field amplitude of an AAF beam is proportional to $J_0(r_0 r/z + r^3/3z^3)$, which is just a Bessel function! Using Eq. (8), the shape of the obtained beam can be controlled through r_0, z, and a.

The previous analysis can be applied to outward accelerating CABs, too. These beams have an input amplitude $Ai(r - r_0)\exp[a(r - r_0)]$, i.e. inward developing intensity rings and, although they are not AAF waves, they have also been studied experimentally and used to produce Bessel-like beams in the far-field [7]. Then, provided that r_0 is sufficiently large, so that the input amplitude near the beam axis is negligible, the FT for $k < \sqrt{r_0}$ is approximated by Eq. (8), with $(r_0 + k^2)$ replaced by $(r_0 - k^2)$ and with k^3 replaced by $-k^3$. Therefore, outward CABs also morph into chirped Bessel-like beams and, inversely, they can be generated by Fourier-transforming such beams.

Let us now use Eq. (8) to design AAF beams. Assume the input amplitude $w(r, 0) = V(r/c)/c$, with $r_0 = c$, where r is the polar distance scaled by the arbitrary length x_0 and c determines the chirp rate. While propagating, the beam passes through a thin lens with focal distance f (scaled by $2\pi x_0^2/\lambda$, λ being the wavelength) positioned at $z = f$. By the lens' FT property, the wave at the back focal plane ($z = 2f$) is given by $-(i/f)W(r/f)$, where W is the FT of $w(r, 0)$. Since V is approximately the FT of the beam of Eq. (1), it follows that

$$w(r, 2f) \cong -i(c/f)Ai(c - cr/f)\exp[a(c - cr/f)], \quad (9)$$

i.e. the beam at the back focal plane is a scaled by c/f CAB with main-ring radius $f + f/c$ and apodization rate a. Ray optics in the half-space $z > f$ show that the paraboloid caustic surface of revolution $r = f - c^3(z - 2f)^2/4f^3$ is formed. For $c > (2f)^{2/3}$, which we term as the *weak-chirp* regime, this caustic collapses at two on-axis points: $z = 2f \mp L$ where $L = 2f^2 c^{-3/2}$ and two foci are created behind the lens. For $c < (2f)^{2/3}$ (*strong-chirp* regime), there is one focus behind the lens and another one in front of it, approximately at $z = (1/2)c^{3/2}$; a result of the collapse of the caustic surface of revolution

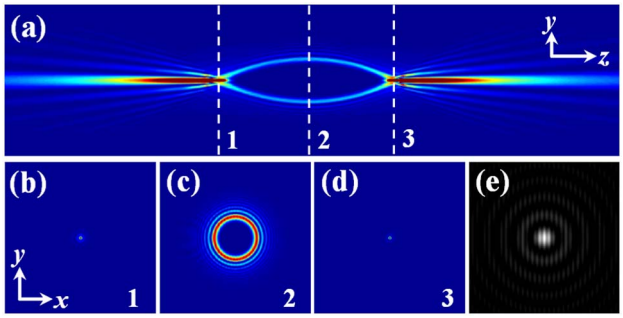

Fig. 2. (Color online) BPM simulation of optical bottle generation from a CAB. (a) Side-view of the bottle beam dynamics numerically retrieved from the computer–generated hologram (e); (b)–(d) Transverse intensity patterns taken at planes 1–3 marked in (a); (e) a typical off-axis hologram.

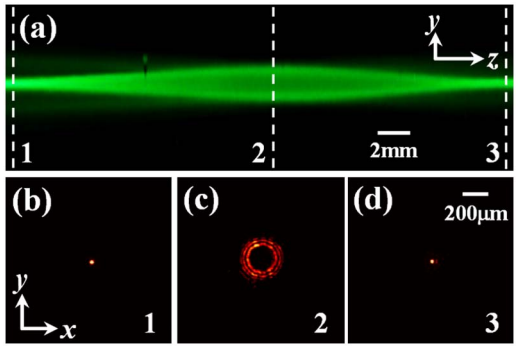

Fig. 3. (Color online) Experimental results of an optical bottle beam generated using the hologram of Fig. 2(e). (a) Side-view photo of the bottle beam taken from scattered light; (b)–(d) transverse intensity snapshots at planes 1–3 marked in (a).

$r = c^3/(4z) - z$, created by the chirped Bessel beam itself.

Examples of these two distinct regimes are shown in Fig. 1, computed numerically using Hankel transforms [1]. In Fig. 1(b), the weak-chirp case, the Bessel-like input beam propagates nearly diffraction-free before the lens. After being focused, it forms a paraboloid caustic surface that collapses at two mirror-symmetric foci, with respect to $z = 2f$. The "defocusing-to-focusing" effect creates an elegant optical bottle with multilayer, paraboloid intensity boundaries and an almost perfect Ai^2 radial dependence. The length and width of the bottle are approximately $2L$ and $2f$, respectively, and can be controlled for optical-trapping applications. On the other hand, in the strong-chirp case of Fig. 1(c), the input beam forms quickly a caustic surface of revolution that collapses to a focus before the lens and then starts to diffract. The diffraction is inhibited by the lens and a parabolic caustic with outward launch angle is created that finally collapses at a single distant focus.

To experimentally verify our theoretical predictions, we employed a setup similar to that used in our previous demonstration of AAF CABs [7]. A spatial light modulator (SLM) was programmed with the off-axis hologram obtained by computing the interference between a plane wave and a Bessel beam with a cubic phase chirp and shown in Fig. 2(e). Then, a Gaussian beam from a Coherent Verdi laser ($\lambda = 532\,\mathrm{nm}$) was sent through the reflection-type SLM (Holoeye LC-R 2500 with 1024× 768 pixels) to retrieve the hologram [9]. The phase-chirped Bessel beam was finally turned into an optical bottle by a FT lens. Beam propagation method (BPM) results corresponding to this arrangement are shown in Fig. 2, illustrating clearly the formation of an optical bottle with multilayer paraboloid boundaries and two closed ends. The experimental results are displayed in Fig. 3, where the side-view photograph of Fig. 3(a) was taken from scattered light and the transverse intensity patterns were recorded directly with a CCD camera. The fine multilayer structure at the bottle waist and two closed ends are clearly visible in Figs. 3(b)–3(d). These observations are in good agreement with the results of BPM (Fig. 2) and with the full-wave simulations (Fig. 1). It should be pointed out that the optical bottle produced this way has two completely closed ends, in contrast to those generated earlier from optical vortex beams [8,9]. Such a perfectly closed bottle might be particularly useful for stable trapping and manipulation of nano- and microsized particles. Note that, as shown by Eq. (9), the size of the generated bottle can be reduced at will (and without losing its mirror symmetry) by employing a FT-lens with a smaller focal distance.

In conclusion, we have set the analytical ground for engineering AAF waves in the Fourier-space and shown how CABs can form elegant paraboloid optical bottles. The theoretical predictions were verified by experimental demonstrations. Our findings reveal a connection between AAF waves and Bessel beams with a nonlinear argument that is a potential starting point for conceiving new ways for generating AAF waves.

This work was supported in part by the Archimedes Center for Modeling, Analysis and Computation (ACMAC) (project FP7-REGPOT-2009-1), and by the United States Air Force Office of Scientific Research (USAFOSR) (grant nos. FA9550-10-1-0561 and FA9550-09-1-0474) and National Science Foundation (NSF) (PHY-0800972).

References

1. N. K. Efremidis and D. N. Christodoulides, Opt. Lett. **35**, 4045 (2010).
2. I. Chremmos, N. K. Efremidis, and D. N. Christodoulides, Opt. Lett. **36**, 1890 (2011).
3. D. G. Papazoglou, N. K. Efremidis, D. N. Christodoulides, and S. Tzortzakis, Opt. Lett. **36**, 1842 (2011).
4. P. Zhang, J. Prakash, Z. Zhang, Y. Hu, N. K. Efremidis, V. Kajorndejnukul, D. Christodoulides, and Z. Chen, in *Quantum Electronics and Laser Science Conference*, OSA Technical Digest (CD) (Optical Society of America, 2011), paper QThS7.
5. G. A. Siviloglou, J. Broky, A. Dogariu, and D. N. Christodoulides, Phys. Rev. Lett. **99**, 213901 (2007).
6. C.-Y. Hwang, K.-Y. Kim, and B. Lee, Opt. Express **19**, 7356 (2011).
7. P. Zhang, J. Prakash, Ze Zhang, M. S. Mills, N. K. Efremidis, D. N. Christodoulides, and Z. Chen, Opt. Lett. **36**, 2883 (2011).
8. V. G. Shvedov, A. S. Desyatnikov, A. V. Rode, W. Krolikowski, and Y. S. Kivshar, Opt. Express **17**, 5743 (2009).
9. P. Zhang, Z. Zhang, J. Prakash, S. Huang, D. Hernandez, M. Salazar, D. N. Christodoulides, and Z. Chen, Opt. Lett. **36**, 1491 (2011).